ChemComm

Accepted Manuscript

This article can be cited before page numbers have been issued, to do this please use: C. Guo, Y. zhang, Y. Guo, L. Zhang, Y. Zhang and J. Wang, *Chem. Commun.*, 2017, DOI: 10.1039/C7CC07698C.

This is an Accepted Manuscript, which has been through the Royal Society of Chemistry peer review process and has been accepted for publication.

Accepted Manuscripts are published online shortly after acceptance, before technical editing, formatting and proof reading. Using this free service, authors can make their results available to the community, in citable form, before we publish the edited article. We will replace this Accepted Manuscript with the edited and formatted Advance Article as soon as it is available.

You can find more information about Accepted Manuscripts in the author guidelines.

Please note that technical editing may introduce minor changes to the text and/or graphics, which may alter content. The journal's standard Terms & Conditions and the ethical guidelines, outlined in our author and reviewer resource centre, still apply. In no event shall the Royal Society of Chemistry be held responsible for any errors or omissions in this Accepted Manuscript or any consequences arising from the use of any information it contains.

ROYAL SOCIETY OF CHEMISTRY

rsc.li/chemcomm

View Article Online
DOI: 10.1039/C7CC07698C

Journal Name

COMMUNICATION

A general and efficient approach for tuning crystal morphology of classical MOFs

Received 00th January 20xx,
Accepted 00th January 20xx

DOI: 10.1039/x0xx00000x

www.rsc.org/

Changyan Guo [a], Yonghong Zhang [a], Yuan Guo [a], Liugen Zhang [a], Yi Zhang [a, b], Jide Wang [a] *

This paper introduces a general approach toward the size/morphology-controlled synthesis of classical MOFs with 2-methylimidazole (2-MI) as a competitive ligand and base to accelerated the nucleation of crystallization. The higher concentration of 2-MI, suitable polarity and solubility of the solvent will accelerating the nucleation of the crystal, resulting in nanometer size particles. While, larger crystals can be obtained via the further growth of nanoparticles with prolonging the reaction time. Such a serendipitous discovery may inspire future researchers to design new MOFs materials with desired structures.

Metal-organic frameworks (MOFs), refer to a class of highly ordered, promising crystalline porous materials composed of inorganic and organic units linked into one-, two-, or three-dimensional networks.[1] Over the past decade, owing to their diverse frameworks, extremely large surface areas, tailorable molecular cavities, feasible post-synthetic modifications, and exceptional thermal and chemical stability,[2] MOFs have been widely applied, including but not limited in gas separation and storage,[3] heterogeneous catalysis,[4] adsorption of organic molecules[5] and drug delivery.[6]

The main researches in this field have been focused on the design, synthesis, characterization, and application of bulk MOF materials,[7] suggesting that the functionalities and utilities of molecular materials are greatly influenced by their chemical composition, size and morphology.[8] Recently, nano-sized MOF materials (NMOFs) have been examined for prospective applications in heterogeneous catalysis, porous membranes, biomedical imaging and controlled drug release.[8a,8c,9] Since NMOFs usually exhibit unique or enhanced properties for easier transportation of guest molecules, short diffusion pathways and exposed active sites within the nano-MOF crystals.[2b,2d,8b] The synthesis of NMOFs with special morphology has proven to be an important factor in extending these materials to more unique, prosperous applications, e.g., gas separation and heterogeneous catalysis.[1d,2d,8a]

To synthesize the size/morphology-controlled MOF crystals usually depends on the precise control over MOF nucleation, growth and the development of procedures to induce MOF formation on specific substrates.[10] To date, several strategies have been developed for the synthesis of nanosized MOFs in the presence of additives. These include: (i) initiation solvent: the solvent-induced precipitation favors fast nucleation and slows the crystal growth rate, resulting in nanometer size particles;[11] (ii) surfactant-assisted synthesis: the surfactant acts as a capping agent or inhibitor during the synthetic process, decreases the surface energy and total system energy via dipole-dipole interactions or van der Waals forces that slow down the crystal growth rate;[2b,8b,12] (iii) hard templates: hard templates can also be used to tune the MOF particle morphology and porosity;[12a,13] (iv) coordination modulation: in some cases, the modulator acts indirectly by altering the acid/base equilibria of either the starting materials or the intermediate species to promote the formation of coordination bonds between the metal ions and organic linkers to fabricate the MOF nanocrystals.[2b,8b,10,14] Despite a growing number of methods for regulating MOFs morphology and size by involving different reagents and templates, most of them are only applicable to specific materials. To develop a general and efficient approach for tuning crystal size and morphology of different MOFs is still needed, which will effectively synthesize size/morphology-controlled MOFs with excellent catalytic or adsorption performances.

Herein, we report a general, rapid, straightforward method to obtain classical MOFs with unusual morphology and size for the first time using 2-MI as a coordination modulator. The nano Co-MOF-74 and HKUST-1 can be obtained in 60% and 80% yields at room temperature for a few minutes, respectively. Control experiments indicated that the crystal nucleation and growth were affected via both coordination and deprotonation equilibria of 2-MI. MOFs with different sizes can be obtained by adjusting the concentration of 2-MI, polarity and solubility of the solvent and reaction time.

Our experimental subsequently convinced that 2-MI could also be used as an effective competition and capping agent to control the morphology and size of Co-MOF-74, MOF-5, HKUST-1, Ni-MOF-74, and H_2N-Fe-MIL-101 crystals, respectively. Powder X-ray diffraction (PXRD) of the MOFs obtained using 2-MI showed

[a] Key Laboratory of Oil and Gas Fine Chemicals, Ministry of Education & Xinjiang Uygur Autonomous Region, College of Chemistry and Chemical Engineering, Xinjiang University, Urumqi, 830046, P. R. China. E-mail: awangjd@sina.cn.
[b] Key Laboratory of Resources Chemistry of Nonferrous Metals (Ministry of Education), College of Chemistry and Chemical Engineering, Central South University, Changsha, 410083, China.

View Article Online
DOI: 10.1039/C7CC07698C

diffraction patterns identical to those of the unregulated samples, which indicated that the MOFs structure was not affected by 2-MI and pure MOFs was obtained (Fig. 1). The scanning electron microscopy (SEM) (Fig. 1) results showed that 2-MI had a pronounced effect on the size and morphology of MOFs. In the absence of 2-MI, the Co-MOF-74 crystals had a flower-like morphology with a diameter of approximately 100 μm (Co-MOF-74-1), which was identical to those synthesized using a classical solvothermal method.[15] In the presence of 4 mM 2-MI, spherical monodispersed microcrystals with an average size of 10 μm were formed, and the spherical crystals stacked with many small hexahedral prisms via aggregation of small nuclei or nanoparticles. A spherical Ni-MOF-74 approximately 2 microns in size was obtained by adding 4 mM 2-MI, and its morphology was more uniform than that of Ni-MOF-74 synthesized without 2-MI. Furthermore, a flaky, two-dimensional MOF-5; HKUST-1 with a size of 10 nm and H_2N-Fe-MIL-101 with a uniform morphology were also obtained via the competitive coordination of 2-MI. All above results indicate that 2-MI is suitable for regulating the size and morphology of MOFs with different metals and structures, and it is a general, straightforward method for the synthesis of nano- or microscale MOFs with excellent performances.

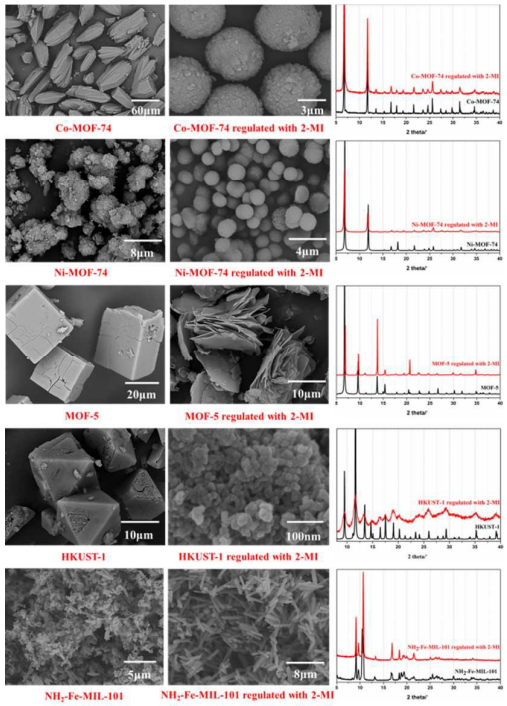

Fig. 1 SEM and PXRD images of Co-MOF-74, Ni-MOF-74, MOF-5, HKUST-1, and H_2N-Fe-MIL-101 without and with regulation by 2-MI.

To further understand the relationship between crystal nucleation and growth with 2-MI in this approach, Co-MOF-74 was selected as a template to study the mechanism of crystal growth. Upon adding 2-MI to a cobalt nitrate solution, the colour of the mixture gradually deepened and became purple (Fig. S1). This result showed that 2-MI was coordinated with Co(II) in MeOH solution.[16] However, when 2,5-dihydroxyterephthalic acid (H_4dhtp) was added to the purple solution, the colour gradually changed until a yellowish-brown precipitate was produced. The same phenomenon was also found in the EtOH and DMF:EtOH:H_2O (1:1:1 v/v/v) solvent systems (Fig. 2), while the crystal growth rate in DMF:EtOH:H_2O (1:1:1 v/v/v) was slower and required incubating or heating. This process was monitored using UV-vis spectroscopy. As shown in Fig. 2, the absorption peak of the $Co(NO_3)_2{\cdot}6H_2O$ solution was located at 518 nm (Fig. 2a). The characteristic peak bathochromic shifted to 540 nm after 2-MI was added, and new absorption peaks located at 587 nm and 658 nm were generated by the coordination of 2-MI with Co(II) (Fig. 2b). When slowly adding H_4dhtp to the mixed solution, the color of the solution gradually became lighter, and the characteristic peak located at 587 nm formed by the coordination effects of the 2-MI with Co(II) rapidly decreased in intensity (Fig. 2c). At the same time, the absorption peak of Co(II) gradually increased, which indicated that the coordination between 2-MI and Co(II) addition was destroyed by adding of H_4dhtp. The coordination absorbs peaks of 2-MI with Co(II) completely disappeared after stirred for 30 min in the presence of 1 mmol H_4dhtp at room temperature (Fig. 2d). The crystal formation in the solution involves nucleation followed by growth.[17] All above results referred to a competitive interaction between H_4dhtp and 2-MI with cobalt ions during the nucleation and crystal growth processes.[18]

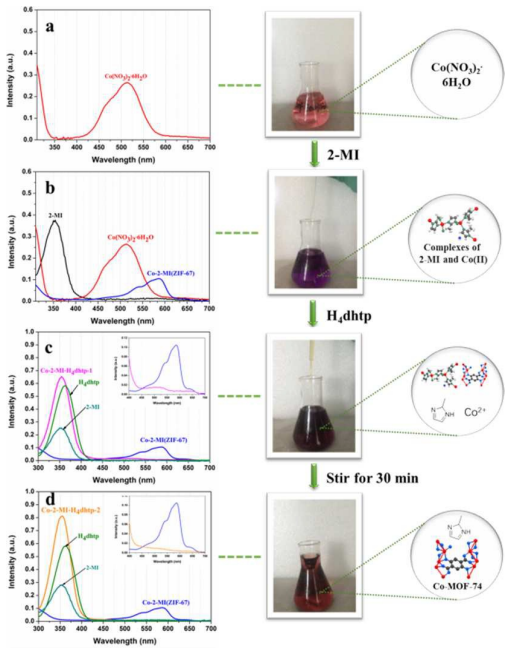

Fig. 2 UV-vis absorption spectra of different samples. a: $Co(NO_3)_2{\cdot}6H_2O$; b: 2-MI was added dropwise to solution a; c: H_4dhtp was added dropwise into solution b; d: solution c was stirred for 30 min at room temperature.

The influence of the reaction conditions on the nucleation and growth of MOFs were monitored to obtain insights into the evolution process of Co-MOF-74 morphologies and sizes. The PXRD (Fig. S2-5) and TEM (Fig. S6) measurements showed that the diffraction patterns obtained with different conditions were identical to the simulated pattern, indicating that pure Co-MOF-74 was formed. The SEM (Fig. S7-11) results clearly indicated that the concentration of 2-MI (Fig. S7), solvents (Fig. S10) and reaction times (Fig. S11) had a deeper influence on the morphology and size of Co-MOF-74, and the size-controlled fabrication was illustrated by Fig. 3. The formation of carboxylate based MOFs is primarily

View Article Online
DOI: 10.1039/C7CC07698C

dependent upon the degree of deprotonation of carboxylic linkers.[2a] In the absence of 2-MI, the degree of deprotonation of H_4dhtp is low, since deprotonation is only depend on the decomposition of DMF to formed dimethyl amine as base at high temperature. In another case, a relatively slow nucleation process is followed by extremely fast particle growth,[7] only bulk Co-MOF-74 in size of about 100 μm was formed. While, in the presence of 2-MI, more deprotonated H_4dhtp ions were available for coordination with metal ions, resulting in increasingly accelerated nucleation rates and therefore decreasing crystal size to approximately 1 μm as the 2-MI concentration increased. The 2-MI not only acts as competitive ligands at the metal centers but also serves as the base for the deprotonation of the bridging ligands. Thus, it will affect crystal nucleation and growth via both coordination and deprotonation equilibria.[8b]

The nucleation rate was accelerated by the addition of 2-MI, the subsequent crystal growth may involve the Ostwald ripening at the expense of metal ions and linkers as well as smaller nanoparticles to yield MOF crystals.[2b] The formation of large particles at the cost of small particles is presumably due to the energy difference between large and small nanoparticles.[8a] Fig. 3 indicated that the DMF was propitious to the dissolution of H_4dhtp and small particles, resulting in the growth of larger particles, and crystals about 10 μm in size can be obtained in DMF:H_2O (1:1 (v/v)) and DMF:MeOH:H_2O (1:1:1 (v/v/v)). In the MeOH:H_2O (1:1 (v/v)), spherical nanocrystals with diameters of 300-500 nm were obtained at room temperature (Co-MOF-74-3). This is because that the increasing of the polarity of solvent facilitates the exchanging between the metal ions and the ligand, and therefore accelerating the nucleation of the crystal. And also, the rapid decrease of supersaturation will reduce the growth of nano nucleus to obtained nanosized crystal.[1f, 19] While, the crystal size decreased to about 20-30 nm at room temperature (Co-MOF-74-4) in MeOH. MeOH is beneficial to accelerate the nucleation of crystal, but not conducive to the rapid dissolution and growth of small nuclei, resulting in smaller crystals. So, the crystals with different sizes can be obtained by adjusting the solvent system. Additionally, when the reaction time was shortened to 10 min, small uniform of spherical crystals were obtained with an average size of 800 nm (Co-MOF-74-2). As the time was prolonged to 12 or 24 h, the increase in particle size could be resulted from further growth via aggregation of small nuclei or nanoparticles which formed extremely fast in the presence of 2-MI.[7, 19] Producing various crystal sizes changed from 800 nm to several micrometers.

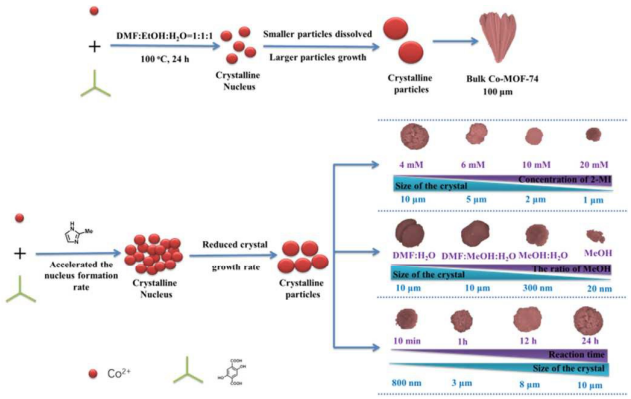

Fig. 3 The evolution process of Co-MOF-74 morphologies and sizes by 2-MI.

TGA experiments were performed on Co-MOF-74 prepared under different conditions. Fig. S12 showed that all four MOFs had similar thermal stabilities, and the crystal structure decomposed higher than 400 °C. Notably, the TGA curves of the Co-MOF-74-2, Co-MOF-74-3 and Co-MOF-74-4 referred to a rapid weight loss before 250 °C, indicating that the solvent molecules in the MOFs obtained via the addition of 2-MI are easily removed and that most of the solvent molecules were removed before 250 °C. This difference could be attributed to the atoms situated on the surface of the small nano-particles have fewer neighbors than the internal atoms, which resulted in a lower binding energy per atom as the particle size decreased. Such feature can be used to effectively remove molecules within the MOF pores, releasing its macropores and providing assistance for gas adsorption and catalysis.

The N_2 adsorption/desorption isotherms of those four types of Co-MOF-74 were type I according to the IUPAC classification of isotherm shapes (Fig. S13),[18b] and this result is in good agreement with the literature.[1e, 15] With the decrease of crystal size, both the specific surface area and pore volume gradually decreased. With the increase of washing times, specific surface area and pore volume increased. However, the average pore size increased, and it may be caused by the presence of hierarchical pores; another reason is because of 2-MI adsorbed in the crystal pores just like the DMF, and with the departure of guest molecules, resulting in an increase in pore size. (Fig. S13a, pore-size distributions calculated using DFT and Horvath-Kawazoe (HK) method can be found in Fig. S14-18). The larger pore size is favorable for the entry and transmission of macromolecules. In catalytic reactions, substrate molecules can be easily introduced into the macropores to perform reactions, and this will improve the contact rate of the substrate and the active sites, which will enhance the catalytic rate and selectivity.

To verify the crystal morphology and size on its application properties, we used the micro- and nanosized crystals prepared by this method for the catalytic oxidation reaction of 2,3-dihydro-1*H*-indene. Table 1 showed that the catalytic conversion of Co-MOF-74-1 obtained by the literature method was 73%. Surprisingly, the conversion of 2,3-dihydro-1*H*-indene to 2,3-dihydro-1*H*-inden-1-one catalyzed by the catalysts (Co-MOF-74-2, Co-MOF-74-3 and Co-MOF-74-4) with smaller sizes and larger pore diameters increased to 90%-93%. The size and morphology of a crystal have a profound impact on its catalytic performance. The large-pore-diameter MOFs exhibit unique or enhanced properties by providing easier transportation of guest molecules and have short diffusion pathways and exposed active sites within the MOF crystals. These

Table 1. Comparison of the catalytic performance for the oxidation of 2,3-dihydro-1*H*-indene.[a]

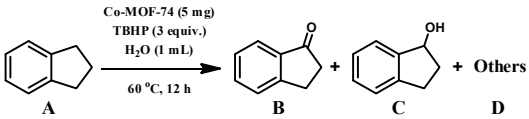

Entry	Catalyst	Conversion (%)	Yield (%)[b]		
			B	C	D
1	Co-MOF-74-1	73	58	12	3
2	Co-MOF-74-2	90	77	8	5
3	Co-MOF-74-3	93	83	6	4
4	Co-MOF-74-4	90	81	6	3

View Article Online
DOI: 10.1039/C7CC07698C

[a] Conditions: **A** (0.2 mmol), catalyst (5 mg), TBHP (0.6 mmol), Solvent (1 mL), 60 °C, 12 h. [b] Conversion and yield were determined by GC.

advantages give the MOFs regulated by 2-MI an excellent catalytic rate and selectivity.

In summary, we have developed a general, rational approach to fabricate size and shape controllable particles from classical MOFs by using 2-MI as a coordination modulator. The nucleation rate was accelerated by the addition of 2-MI via both coordination and deprotonation equilibria, and the crystal size of Co-MOF-74 decreased with increasing of the 2-MI concentration. In addition, the crystal size can be adjusted by controlling the polarity and solubility of the solvent and the reaction time. The TGA test and N_2 adsorption/desorption isotherms results indicated that the Co-MOF-74 obtained by the addition of 2-MI provided better catalytic potential due to the solvent molecules within the Co-MOF-74 pores were easily removed, and their larger pore size, which is favourable to the entry and transmission of macromolecules. This conclusion was confirmed by further catalytic experiments, and the regulated catalysts have better catalytic performance than that of the crystals synthesized using the literature method. We believe that this approach will serve as a useful archetypical template to develop other carboxylate-based MOF crystals with better performances in heterogeneous catalysis.

This work is supported by the National Natural Science Foundation of China (Grant No. 21162027 and 21261022).

Conflicts of interest

There are no conflicts to declare.

Notes and references

1 (a) A. Schoedel, M. Li, D. Li, M. O'Keeffe and O. M. Yaghi, *Chem. Rev.*, 2016**, 116,** 12466-12535; (b) H. Wang, Q. Wang, S. J. Teat, D. H. Olson and J. Li, *Cryst. Growth Des*., 2017**, 17,** 2034-2040; (c) Y. Chen, V. Lykourinou, C. Vetromile, T. Hoang, L. J. Ming, R. W. Larsen and S. Ma, *J. Am. Chem. Soc.*, 2012**, 134,** 13188-13191; (d) K. Liang, R. Ricco, C. M. Doherty, M. J. Styles and P. Falcaro, *CrystEngComm.*, 2016**, 18,** 4264-4267; (e) M. Díaz-García, Á. Mayoral, I. Díaz and M. Sánchez-Sánchez, *Cryst. Growth Des.*, 2014**, 14,** 2479-2487; (f) E. S. Sanil, K.-H. Cho, S.-K. Lee, U. H. Lee, S. G. Ryu, H. W. Lee, J.-S. Chang and Y. K. Hwang, *J. Porous Mat.*, 2015**, 22,** 171-178; (g) S. Sorribas, B. Zornoza, P. Serra-Crespo, J. Gascon, F. Kapteijn, C. Téllez and J. Coronas, *Micropor. Mesopor. Mat.*, 2016**, 225,** 116-121.

2 (a) D. Li, H. Wang, X. Zhang, H. Sun, X. Dai, Y. Yang, L. Ran, X. Li, X. Ma and D. Gao, *Cryst. Growth Des.*, 2014**, 14,** 5856-5864; (b) M.-H. Pham, G.-T. Vuong, A.-T. Vu and T.-O. Do, *Langmuir*, 2011**, 27,** 15261-15267; (c) P. Sarawade, H. Tan and V. Polshettiwar, *ACS Sustain. Chem. Eng.*, 2013**, 1,** 66-74; (d) J.-M. Yang, Q. Liu and W.-Y. Sun, *Micropor. Mesopor. Mat.*, 2014**, 190,** 26-31;

3 (a) S. Ma, D. Sun, J. M. Simmons, C. D. Collier, D. Yuan and H.-C. Zhou, *J. Am. Chem. Soc.*, 2008**, 130,** 1012-1016; (b) H. Furukawa, N. Ko, Y. B. Go, N. Aratani, S. B. Choi, E. Choi, A. Ö. Yazaydin, R. Q. Snurr, M. O'Keeffe, J. Kim and O. M. Yaghi, *Science*, 2010**, 329,** 424; (c) J. Liu, D. M. Strachan and P. K. Thallapally, *Chem. Commun.*, 2014**, 50,** 466-468.

4 (a) B. Yuan, Y. Pan, Y. Li, B. Yin and H. Jiang, *Angew. Chem. Int. Ed.*, 2010**, 49**, 4054-4058; (b) 16 H. L. Jiang, T. Akita, T. Ishida, M. Haruta and Q. Xu, *J. Am. Chem. Soc.*, 2011**, 133,** 1304-1306; (c) M. Zhang, J. Guan, B. Zhang, D. Su, C. T. Williams and C. Liang, *Catal. Lett.*, 2012**, 142,** 313-318.

5 (a) T. K. Trung, P. Trens, N. Tanchoux, S. Bourrelly, P. L. Llewellyn, S. Loera-Serna, C. Serre, T. Loiseau, F. Fajula and G. Férey, *J. Am. Chem. Soc.*, 2008**, 130,** 16926-16932; (b) K. A. Cychosz, A. G. Wong-Foy and A. J. Matzger, *J. Am. Chem. Soc.*, 2008**, 130,** 6938-6939.

6 J. An, S. J. Geib and N. L. Rosi, *J. Am. Chem. Soc.*, 2009**, 131,** 8376-8377.

7 H. Guo, Y. Zhu, S. Wang, S. Su, L. Zhou and H. Zhang, *Chem. Mater.*, 2012**, 24,** 444-450.

8 (a) N. Shi, D. Xu, X. Zhou, L. Song, L. Li, L. Xie, L. Wang, M. Yi and W. Huang, *CrystEngComm.*, 2016**, 18,** 4830-4835; (b) H. Bunzen, M. Grzywa, M. Hambach, S. Spirkl and D. Volkmer, *Cryst. Growth Des.*, 2016**, 16,** 3190-3197; (c) M. O'Keeffe, M. A. Peskov, S. J. Ramsden and O. M. Yaghi, *Acc. Chem. Res.*, 2008**, 41,** 1782-1789.

9 (a) M. Pang, A. J. Cairns, Y. Liu, Y. Belmabkhout, H. C. Zeng and M. Eddaoudi, *J. Am. Chem. Soc.*, 2012**, 134,** 13176-13179; (b) N. Stock and S. Biswas, *Chem. Rev.*, 2012**, 112,** 933-969; (c) N. Yanai and S. Granick, *Angew. Chem. Int. Ed.*, 2012**, 51,** 5638-5641; (d) Y. Pan, D. Heryadi, F. Zhou, L. Zhao, G. Lestari, H. Su and Z. Lai, *CrystEngComm.*, 2011**, 13,** 6937-6940.

10 C. M. Doherty, D. Buso, A. J. Hill, S. Furukawa, S. Kitagawa and P. Falcaro, *Acc. Chem. Res.*, 2014**, 47,** 396-405.

11 (a) X. Cheng, A. Zhang, K. Hou, M. Liu, Y. Wang, C. Song, G. Zhang and X. Guo, *Dalton Trans.*, 2013**, 42,** 13698-13705; (b) B. Seoane, S. Castellanos, A. Dikhtiarenko, F. Kapteijn and J. Gascon, Coord. *Chem. Rev.*, 2016**, 307,** 147-187.

12 (a) J. Cravillon, R. Nayuk, S. Springer, A. Feldhoff, K. Huber and M. Wiebcke, *Chem. Mater.*, 2011**, 23,** 2130-2141; (b) C. He, D. Liu and W. Lin, *Chem. Rev.*, 2015**, 115,** 11079-11108.

13 (a) P. Hu, J. Zhuang, L.-Y. Chou, H. K. Lee, X. Y. Ling, Y.-C. Chuang and C.-K. Tsung, *J. Am. Chem. Soc.*, 2014**, 136,** 10561-10564; (b) H. Kim, M. Oh, D. Kim, J. Park, J. Seong, S. K. Kwak and M. S. Lah, *Chem. Commun.*, 2015**, 51,** 3678-3681.

14 (a) J.-M. Yang, Z.-P. Qi, Y.-S. Kang, Q. Liu and W.-Y. Sun, *Micropor. Mesopor. Mat.*, 2016**, 222,** 27-32; (b) D. Zacher, R. Nayuk, R. Schweins, R. A. Fischer and K. Huber, *Cryst. Growth Des.*, 2014**, 14,** 4859-4863.

15 H. Jiang, Q. Wang, H. Wang, Y. Chen and M. Zhang, *Catal. Commun.*, 2016**, 80,** 24-27.

16 S. Diring, S. Furukawa, Y. Takashima, T. Tsuruoka and S. Kitagawa, *Chem. Mater.*, 2010**, 22,** 4531-4538.

17 N. Yanai, M. Sindoro, J. Yan and S. Granick, *J. Am. Chem. Soc.*, 2013**, 135,** 34-37.

18 (a) M. R. Armstrong, S. Senthilnathan, C. J. Balzer, B. Shan, L. Chen and B. Mu, *Ultrason. Sonochem.*, 2017**, 34,** 365-370; (b) K. S. W. Sing, *Pure Appl. Chem.*, 1985**, 57,** 603-619; (c) Z. Jiang, Z. Li, Z. Qin, H. Sun, X. Jiao and D. Chen, *Nanoscale*, 2013**, 5,** 11770-11775.

19 P. Sarawade, H. Tan, D. Anjum, D. Cha, V. Polshettiwar, ChemSusChem., 2014**, 7,** 529-535.